



Mass transfer coefficient and concentration boundary layer thickness for a dissolving NAPL pool in porous media

Constantinos V. Chrysikopoulos^{a,*}, Pin-Yi Hsuan^a,
Marios M. Fyrillas^b, Kenneth Y. Lee^c

^a *Department of Civil and Environmental Engineering, University of California, Irvine, CA 92697, USA*

^b *Department of Mechanical and Aerospace Engineering, University of California at San Diego, La Jolla, CA 92093, USA*

^c *Department of Civil and Environmental Engineering Rutgers, The State University of New Jersey, Piscataway, NJ 08854, USA*

Received 23 May 2002; received in revised form 26 September 2002; accepted 27 September 2002

Abstract

Analytical expressions for the time invariant, average mass transfer coefficient and the concentration boundary layer thickness applicable to dissolving single-component nonaqueous phase liquid (NAPL) pools in two-dimensional, saturated, homogeneous and isotropic porous formations are derived. Good agreement between predicted and experimentally determined time invariant average mass transfer coefficients is observed.

© 2002 Elsevier Science B.V. All rights reserved.

Keywords: NAPL pool dissolution; Mass transfer coefficient; Concentration boundary layer; Contaminant transport; Analytical solutions

1. Introduction

Subsurface formations are often contaminated by nonaqueous phase liquids (NAPLs) originating from leaking underground storage tanks, ruptured pipelines, surface spills, hazardous waste landfills, disposal sites, and leachates from recycled wastes [19]. When a NAPL spill infiltrates a subsurface formation through the vadose zone, a portion of it may be trapped and immobilized within the unsaturated porous formation in the form of blobs

* Corresponding author. Tel.: +1-949-824-8661; fax: +1-949-824-3672.
E-mail address: costas@eng.uci.edu (C.V. Chrysikopoulos).

Nomenclature

C	aqueous-phase concentration (solute mass/aqueous volume, M/L^3)
C_b	background (free stream) aqueous-phase concentration (M/L^3)
C_s	aqueous saturation concentration (solubility, M/L^3)
D_x	longitudinal hydrodynamic dispersion coefficient (L^2/T)
D_z	hydrodynamic dispersion coefficient in the vertical direction (L^2/T)
\mathcal{D}	molecular diffusion coefficient (L^2/T)
\mathcal{D}_e	effective molecular diffusion coefficient, equal to \mathcal{D}/τ^* (L^2/T)
k	time invariant local mass transfer coefficient (L/T)
k^*	time invariant average mass transfer coefficient (L/T)
K_d	distribution coefficient (L^3/M)
ℓ_x	pool length along the x direction (L)
U_x	average interstitial fluid velocity (L/T)
x	spatial coordinate (L)
y	spatial coordinate (L)

Greek symbols

δ_c	concentration boundary layer thickness (L)
θ	porosity (liquid volume/aquifer volume, L^3/L^3)
λ	decay coefficient for the aqueous-phase concentration (T^{-1})
λ^*	decay coefficient for the concentration sorbed onto the solid matrix (T^{-1})
ξ	dummy integration variable
ρ	bulk density of the porous medium (M/L^3)
τ^*	tortuosity factor (≥ 1)

or ganglia. Upon reaching the water table, dense nonaqueous phase liquids (DNAPLs) with densities heavier than that of water (sinkers, e.g. organic leachates from recycled hazardous solid wastes), given that the pressure head at the capillary fringe is sufficiently large, continue to migrate downward leaving behind trapped ganglia until they encounter an impermeable layer, where a flat source zone or pool starts to form [30]. NAPLs with densities lower than that of water (floaters, e.g. petroleum products) as soon as they reach the saturated region, spread laterally and float on the water table in the form of a pool [29]. As groundwater flows past trapped ganglia or NAPL pools, a fraction of the NAPL dissolves in the aqueous phase and a plume of dissolved hydrocarbons is created.

The aqueous-phase concentrations of dissolved NAPLs in groundwater are primarily governed by interphase mass transfer processes that often are slow and rate-limited [25]. Furthermore, the dissolution of NAPL pools in porous media is fundamentally different from that of residual blobs [6]. NAPL pools have limited contact areas with respect to groundwater. If the same volume of a NAPL is present as ganglia and as pool, ganglia dissolution is expected to proceed at a faster rate, because of the larger surface area available for interphase mass transfer [29]. Consequently, NAPL pools often lead to long-lasting sources of groundwater contamination.

Numerous studies have focused on the migration and dissolution of residual blobs [1,5,16,18,33,34], as well as on the dissolution of NAPL pools [3,10,13,17,21,22,24,26,30–32]. Furthermore, several theoretically and experimentally derived mass transfer relationships for the dissolution of residual NAPL blobs [15,28] and NAPL pools [8,12,20,23] have been presented in the literature.

Mathematical models for contaminant transport originating from NAPL pool dissolution often assume that the dissolution process is instantaneous when mass transfer rates at the NAPL–water interface are much faster than the advective-dispersive transport of the dissolved NAPLs away from the interface, and employ average and time invariant mass transfer coefficients which are representative of the entire pool [6,14]. In this work, analytical relationships for the average mass transfer coefficient and the concentration boundary layer thickness applicable to dissolving NAPL pools in two-dimensional, homogeneous subsurface formations under steady-state conditions are derived.

2. Mathematical formulation

The task of obtaining analytical expressions for mass transfer coefficients applicable to a dissolving NAPL pool in water saturated porous media is not trivial. However, for relatively simple cases of well-defined NAPL pool geometries under ideal conditions, analytical expressions for mass transfer coefficients can be derived. For example, consider a single-component NAPL pool that is denser than water and is formed on top of a low permeability layer within a two-dimensional, saturated, homogeneous and isotropic porous medium. The steady-state transport of the dissolving NAPL into the aqueous phase under uniform flow conditions is governed by

$$U_x \frac{\partial C(x, z)}{\partial x} = D_x \frac{\partial^2 C(x, z)}{\partial x^2} + D_z \frac{\partial^2 C(x, z)}{\partial z^2} - \lambda C(x, z) - \lambda^* \frac{\rho}{\theta} K_d C(x, z), \quad (1)$$

where $C(x, z)$ is the aqueous-phase solute concentration, x, z the spatial coordinates in the longitudinal and vertical (perpendicular to the interface) directions, respectively, U_x the average interstitial fluid velocity, D_x and D_z are the longitudinal and vertical hydrodynamic dispersion coefficients, respectively, λ is the first-order decay coefficient of the aqueous-phase concentration, λ^* the first-order decay coefficient of the concentration sorbed onto the solid matrix, ρ the bulk density of the solid matrix, θ the porosity of the porous medium, and K_d is the partition or distribution coefficient.

For mathematical simplicity, it is hypothesized that the sorption of the dissolved NAPL can be described by a linear equilibrium isotherm and that the local chemical equilibrium assumption is valid. Furthermore, the last two terms on the right-hand side of the governing Eq. (1) account for decay due to possible biological/chemical degradation of the aqueous-phase concentration and the concentration sorbed onto the solid matrix. Although the direct inter-relationship between sorption of halogenated compounds onto solids and biotransformation has yet to be thoroughly examined, experimental evidence suggests that organic solutes undergo degradation primarily in the aqueous phase [2,27]. Therefore, in order to make the present model general, two different decay coefficients are employed.

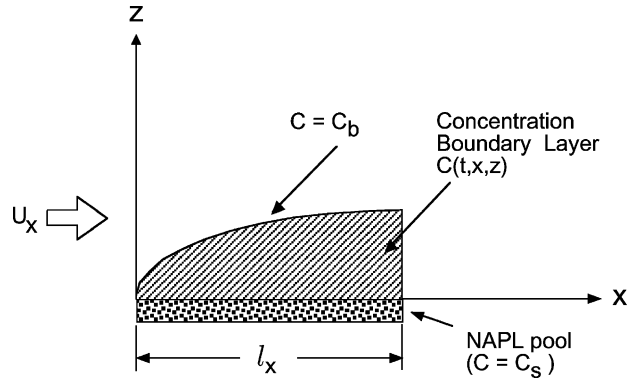


Fig. 1. Schematic illustration of the conceptual model showing a NAPL pool with length ℓ_x within a porous formation under unidirectional interstitial velocity U_x . The concentration within the boundary layer decreases from saturation concentration, C_s , at the NAPL–water interface to background concentration, C_b , in the bulk interstitial liquid.

To further simplify the physical system we assume that advective transport is much greater than the corresponding dispersive transport along the x direction ($U_x \gg D_x$). For this limiting case the governing Eq. (1) reduces to

$$U_x \frac{\partial C(x, z)}{\partial x} = D_z \frac{\partial^2 C(x, z)}{\partial z^2} - \lambda C(x, z) - \lambda^* \frac{\rho}{\theta} K_d C(x, z). \quad (2)$$

For the system examined here, as illustrated in Fig. 1, the appropriate initial and boundary conditions are:

$$C(0, z) = 0, \quad (3)$$

$$C(x, 0) = C_s, \quad (4)$$

$$C(x, \infty) = 0, \quad (5)$$

where C_s is the aqueous saturation (solubility) concentration of the dissolved NAPL at the NAPL–water interface. The solution to (2) subject to conditions (3)–(5) is obtained by straightforward Laplace transform procedures to yield

$$\begin{aligned} C(x, z) = & \frac{C_s}{2} \exp \left[\frac{z}{D_z^{1/2}} \left(\lambda + \lambda^* \frac{\rho}{\theta} K_d \right)^{1/2} \right] \\ & \times \operatorname{erfc} \left\{ \frac{z}{2} \left(\frac{U_x}{D_z x} \right)^{1/2} + \left[\frac{x}{U_x} \left(\lambda + \lambda^* \frac{\rho}{\theta} K_d \right) \right]^{1/2} \right\} \\ & + \frac{C_s}{2} \exp \left[-\frac{z}{D_z^{1/2}} \left(\lambda + \lambda^* \frac{\rho}{\theta} K_d \right)^{1/2} \right] \\ & \times \operatorname{erfc} \left\{ \frac{z}{2} \left(\frac{U_x}{D_z x} \right)^{1/2} - \left[\frac{x}{U_x} \left(\lambda + \lambda^* \frac{\rho}{\theta} K_d \right) \right]^{1/2} \right\}, \quad (6) \end{aligned}$$

where $\text{erfc}[\cdot]$ is the complementary error function defined as

$$\text{erfc}[\eta] = 1 - \text{erf}[\eta] = 1 - \frac{2}{\pi^{1/2}} \int_0^\eta \exp[-\xi^2] d\xi, \quad (7)$$

$\text{erf}[\cdot]$ is the error function, and ξ is a dummy integration variable. The analytical solution (6) can be used to predict aqueous-phase concentrations resulting from NAPL pool dissolution in a two-dimensional aquifer at steady-state conditions. For the special case where the dissolved NAPL concentration is conservative the two first-order decay coefficients are equal to zero ($\lambda = \lambda^* = 0$) and (6) reduces to the familiar expression:

$$C(x, z) = C_s \text{erfc} \left[\frac{z}{2} \left(\frac{U_x}{D_z x} \right)^{1/2} \right]. \quad (8)$$

The preceding expression for the aqueous-phase concentration is independent of K_d , because at steady-state conditions the magnitude of K_d (or equivalently the retardation factor) does not affect the dissolved NAPL concentration in the homogeneous aquifer when $\lambda = \lambda^* = 0$ [9].

3. Time invariant average mass transfer coefficient

The mass flux from a NAPL–water interface into the aqueous interstitial fluid within a water saturated, two-dimensional, homogeneous porous formation is described by the following relationship [9]:

$$-D_e \left. \frac{\partial C(x, z)}{\partial z} \right|_{z \rightarrow 0} = k(x)[C_s - C(x, \infty)], \quad (9)$$

where $D_e = D/\tau^*$ is the effective molecular diffusion coefficient (where D is the molecular diffusion coefficient, and $\tau^* \geq 1$ is the tortuosity coefficient), and k is the time invariant local mass transfer coefficient. Conventionally, any location above the concentration boundary layer is considered as $z \rightarrow \infty$. For the case where the background concentration is constant with respect to time and space, for notational convenience, $C(x, \infty)$ is replaced by C_b , the constant background aqueous-phase concentration. It should be noted that in this study the free stream concentration is assumed to be zero ($C_b = 0$). The mass transfer relationship (9) implies that the dissolution at the NAPL–water interface is limited only by mass transfer. The concentration along the interface is assumed constant and equal to the saturation concentration, $C(x, 0) = C_s$. For a NAPL–water interfacial area with finite length, in view of (9), the appropriate expression for the time invariant average mass transfer coefficient is given by

$$k^* = -\frac{D_e}{\ell_x C_s} \int_0^{\ell_x} \left. \frac{\partial C(\xi, z)}{\partial z} \right|_{z \rightarrow 0} d\xi, \quad (10)$$

where ℓ_x is the NAPL pool dimension in x direction as shown in Fig. 1.

Differentiating (6) with respect to z and taking the limit $z \rightarrow 0$ yields

$$\begin{aligned} \left. \frac{\partial C(x, z)}{\partial z} \right|_{z \rightarrow 0} &= -C_s \left[\frac{1}{D_z} \left(\lambda + \lambda^* \frac{\rho}{\theta} K_d \right) \right]^{1/2} \operatorname{erf} \left\{ \left[\frac{x}{U_x} \left(\lambda + \lambda^* \frac{\rho}{\theta} K_d \right) \right]^{1/2} \right\} \\ &\quad - C_s \left(\frac{U_x}{\pi D_z x} \right)^{1/2} \exp \left[-\frac{x}{U_x} \left(\lambda + \lambda^* \frac{\rho}{\theta} K_d \right) \right]. \end{aligned} \quad (11)$$

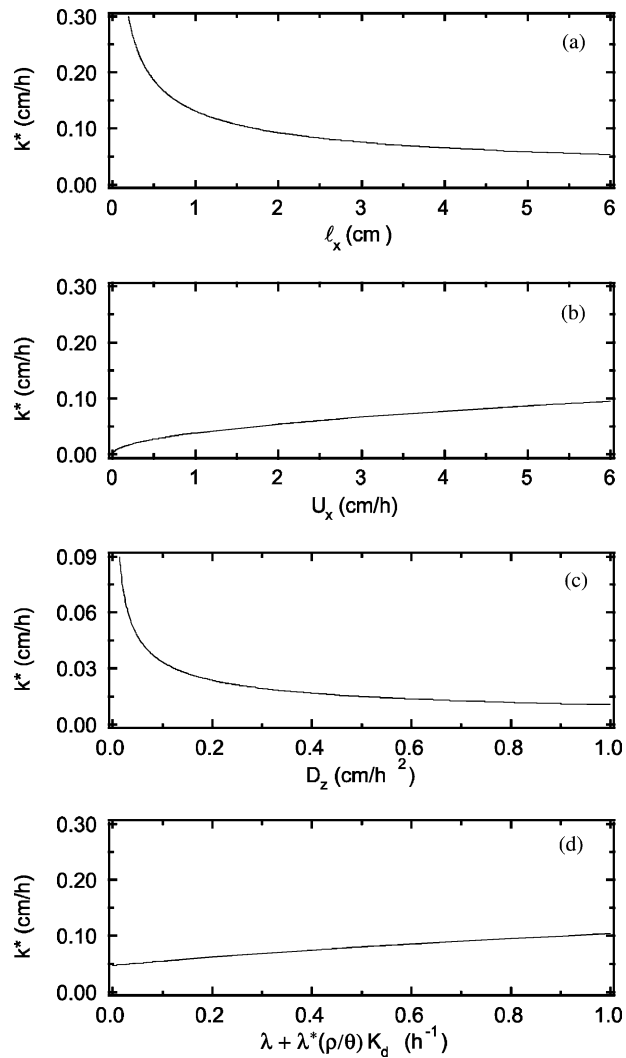


Fig. 2. Variation of the time invariant overall mass transfer coefficient as a function of (a) pool length, (b) interstitial velocity, (c) vertical hydrodynamic dispersion coefficient, and (d) overall decay coefficient (here $\ell_x = 7.7$ cm, $U_x = 1.5$ cm/h, $D_z = 0.05$ cm²/h, and $\lambda = \lambda^* = 0$ h⁻¹).

Substituting (11) into (10) and integrating enables us to obtain the desired expression for the time invariant average mass transfer coefficient

$$k^* = \frac{D_e}{\ell_x} \left[\frac{U_x}{2D_z^{1/2}} \left(\lambda + \lambda^* \frac{\rho}{\theta} K_d \right)^{-1/2} + \frac{\ell_x}{D_z^{1/2}} \left(\lambda + \lambda^* \frac{\rho}{\theta} K_d \right)^{1/2} \right] \\ \times \operatorname{erf} \left\{ \left[\frac{\ell_x}{U_x} \left(\lambda + \lambda^* \frac{\rho}{\theta} K_d \right) \right]^{1/2} \right\} + \left(\frac{D_e^2 U_x}{\pi D_z \ell_x} \right)^{1/2} \exp \left[-\frac{\ell_x}{U_x} \left(\lambda + \lambda^* \frac{\rho}{\theta} K_d \right) \right]. \quad (12)$$

For the special case where the aqueous-phase NAPL concentration is conservative both λ and λ^* are equal to zero, and the preceding expression for k^* is simplified to

$$k^* = 2D_e \left(\frac{U_x}{\pi D_z \ell_x} \right)^{1/2}. \quad (13)$$

The sensitivity of the time invariant average mass transfer coefficient to its various model parameters, as predicted by (12), is illustrated in Fig. 2. It is shown in Fig. 2a that k^* decreases exponentially with increasing NAPL pool length. This behavior is expected because k^* represents the integral of the local mass transfer coefficient over the entire NAPL–water interface. It should be noted that the local mass transfer coefficient decreases with distance from the front end of the NAPL pool and has a maximum value at the leading or upstream edge [7]. Fig. 2b indicates that k^* is proportional to the interstitial fluid velocity. This behavior is attributed to increasing concentration gradients at the NAPL–water interface with increasing U_x . Fig. 2c shows that k^* decreases exponentially with increasing D_z . Enhancing the vertical spreading of the aqueous-phase concentration yields to smoother concentration gradients at the NAPL–water interface and consequently to smaller k^* . Fig. 2d indicates that k^* is directly proportional to the overall decay coefficient which is defined here as $\lambda + \lambda^* \rho (K_d/\theta)$. Increasing the decay rate of the aqueous-phase and sorbed concentrations

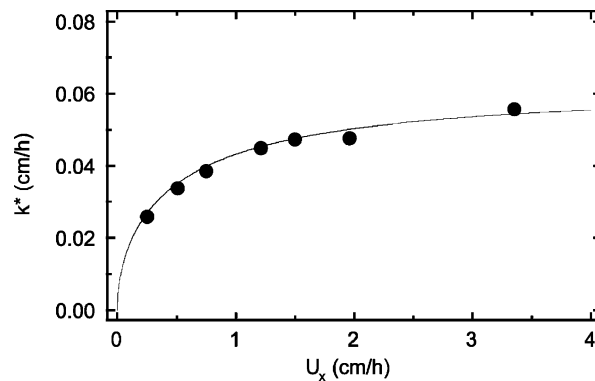


Fig. 3. Comparison between experimentally determined (solid circles) and analytically predicted (solid curve) time invariant average mass transfer coefficients. The experimental data are adapted from [11].

leads to steeper concentration gradients at the NAPL–water interface and consequently to greater k^* .

A favorable comparison between available, experimentally determined time invariant average mass transfer coefficients for seven different interstitial velocities associated with the dissolution of a TCE pool in a water saturated bench-scale aquifer [10,11,23] and those predicted by (12) is presented in Fig. 3. Therefore, the analytical expression for k^* derived in this study may be useful for NAPL pool dissolution investigations where experimental data or pertinent mass transfer coefficient correlations are not available.

4. Concentration boundary layer thickness

The concentration boundary layer thickness, δ_c , is defined as the vertical distance from the NAPL–water interface where the aqueous-phase concentration C is 1% of the saturation concentration C_s ($C = 0.01C_s$) [4]. For the case where $\lambda = \lambda^* = 0$, $z = \delta_c$ and $C/C_s = 0.01$, the analytical solution (6) can be written as

$$0.01 = \operatorname{erfc} \left[\frac{\delta_c}{2} \left(\frac{U_x}{D_z x} \right)^{1/2} \right] = 1 - \operatorname{erf} \left[\frac{\delta_c}{2} \left(\frac{U_x}{D_z x} \right)^{1/2} \right], \quad (14)$$

where the latter formulation is a consequence of (7). The preceding relationship is valid only when the argument of the error function is equal to

$$\frac{\delta_c}{2} \left(\frac{U_x}{D_z x} \right)^{1/2} = 1.82 \approx 2. \quad (15)$$

Solving for δ_c yields the following expression for the boundary layer thickness resulting from a conservative dissolving NAPL pool in a two-dimensional, homogeneous, water saturated porous formation

$$\delta_c \approx 4 \left(\frac{D_z x}{U_x} \right)^{1/2}. \quad (16)$$

Although (16) is an approximate expression, it describes the relationship between the concentration boundary thickness and its associated parameters.

The behavior of δ_c as a function of the various transport parameters is demonstrated graphically in Fig. 4. The concentration boundary layer grows steadily as the longitudinal distance from the source increases (Fig. 4a). This is attributed to the progressive dispersion of the dissolved concentration as it is carried by the moving interstitial fluid. A decrease in δ_c is observed with increasing U_x (Fig. 4b). This is an intuitive result because increasing U_x leads to steeper concentration gradients at the NAPL–water interface. Finally, δ_c is shown to increase with increasing D_z (Fig. 4c) due to the associated increase in vertical spreading of the aqueous-phase concentration. Furthermore, it is evident from Fig. 4 that under typical groundwater conditions δ_c is just a few centimeters thick.

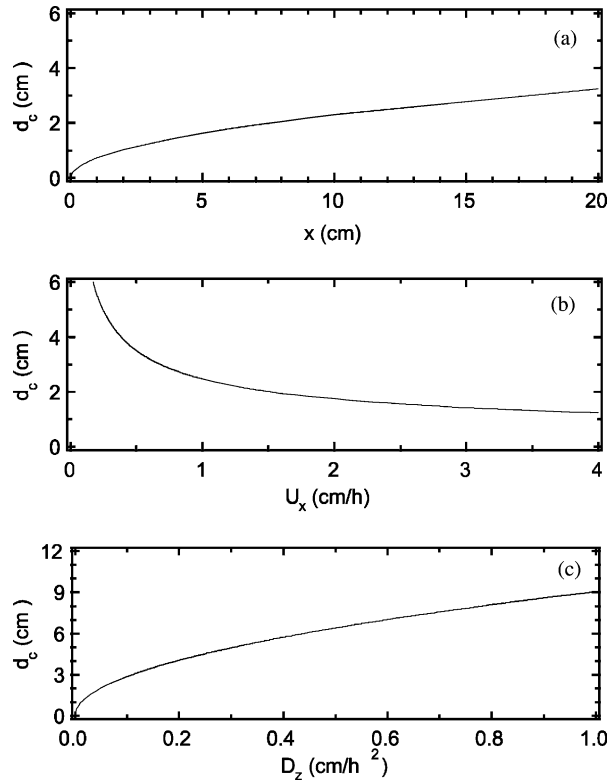


Fig. 4. Predicted concentration boundary layer as a function of (a) longitudinal distance from the source, (b) interstitial velocity, and (c) vertical hydrodynamic dispersion coefficient (here $x = 7.7$ cm, $U_x = 1.5$ cm/h, $D_z = 0.05$ cm²/h, and $\lambda = \lambda^* = 0$ h⁻¹).

5. Summary

Analytical expressions for the time invariant average mass transfer coefficient and for the concentration boundary layer thickness associated with the dissolution of a NAPL pool in two-dimensional porous media were derived. It was demonstrated that δ_c increases with increasing x and D_z , and decreases with increasing U_x . The analytical expression for k^* (12) may be useful to NAPL pool dissolution studies where experimentally determined mass transfer coefficients are not available. The analytical expression for δ_c (16) may be employed in experimental studies of NAPL pool dissolution where appropriate sampling locations for aqueous-phase concentration measurements are desired.

References

- [1] L.M. Abriola, G.F. Pinder, A multiphase approach to the modeling of porous media contamination by organic compounds. 1. Equation development, *Water Resour. Res.* 21 (1) (1985) 11–18.

- [2] L. Alvarez-Cohen, P.L. McCarthy, P.V. Roberts, Sorption of trichloroethylene onto a zeolite accompanied by methanotrophic biotransformation, *Environ. Sci. Technol.* 27 (1993) 2141–2148.
- [3] M.R. Anderson, R.L. Johnson, J.F. Pankow, Dissolution of dense chlorinated solvents into groundwater. 3. Modeling contaminant plumes from fingers and pools of solvent, *Environ. Sci. Technol.* 26 (5) (1992) 901–908.
- [4] R.B. Bird, W.E. Stewart, E.N. Lightfoot, *Transport Phenomena*, Wiley, New York, 1960, 780 pp.
- [5] M.L. Brusseau, N.T. Nelson, M. Oostrom, Z. Zhang, G.R. Johnson, T.W. Wietsma, Influence of heterogeneity and sampling method on aqueous concentrations associated with NAPL dissolution, *Environ. Sci. Technol.* 34 (2000) 3657–3664.
- [6] C.V. Chrysikopoulos, Three-dimensional analytical models of contaminant transport from nonaqueous phase liquid pool dissolution in saturated subsurface formations, *Water Resour. Res.* 31 (4) (1995) 1137–1145.
- [7] C.V. Chrysikopoulos, K.Y. Lee, Contaminant transport resulting from multicomponent nonaqueous phase liquid pool dissolution in three-dimensional subsurface formations, *J. Contam. Hydrol.* 31 (1998) 1–21.
- [8] C.V. Chrysikopoulos, T.-J. Kim, Local mass transfer correlations for nonaqueous phase liquid pool dissolution in saturated porous media, *Transpl. Porous Media* 38 (1–2) (2000) 167–187.
- [9] C.V. Chrysikopoulos, E.A. Voudrias, M.M. Fyrrillas, Modeling of contaminant transport resulting from dissolution of nonaqueous phase liquid pools in saturated porous media, *Transpl. Porous Media* 16 (2) (1994) 125–145.
- [10] C.V. Chrysikopoulos, K.Y. Lee, T.C. Harmon, Dissolution of a well-defined trichloro-ethylene pool in saturated porous media: experimental design and aquifer characterization, *Water Resour. Res.* 36 (7) (2000) 1687–1696.
- [11] C.V. Chrysikopoulos, P.-Y. Hsuan, M.M. Fyrrillas, Bootstrap estimation of the mass transfer coefficient of a dissolving nonaqueous phase liquid pool in porous media, *Water Resour. Res.* 38 (3) (2002) 10.1029/2001WR000661.
- [12] B.K. Dela Barre, T.C. Harmon, C.V. Chrysikopoulos, Measuring and modeling the dissolution of nonideally shaped dense nonaqueous phase liquid (NAPL) pools in saturated porous media, *Water Resour. Res.* 38 (8) (2002) 10.1029/2001WR000444.
- [13] M.M. Fyrrillas, Advection-dispersion mass transport associated with a non-aqueous-phase liquid pool, *J. Fluid Mech.* 413 (2000) 49–63.
- [14] H.-Y.N. Holman, I. Javandel, Evaluation of transient dissolution of slightly water-soluble compounds from a light nonaqueous phase liquid pool, *Water Resour. Res.* 32 (4) (1996) 915–923.
- [15] P.T. Imhoff, P.R. Jaffé, G.F. Pinder, An experimental study of complete dissolution of a nonaqueous phase liquid in saturated porous media, *Water Resour. Res.* 30 (1994) 307–320.
- [16] C. Jia, K. Shing, Y.C. Yortsos, Advective mass transfer from stationary sources in porous media, *Water Resour. Res.* 35 (11) (1999) 3239–3251.
- [17] R.L. Johnson, J.F. Pankow, Dissolution of dense chlorinated solvents into groundwater. 2. Source functions for pools of solvent, *Environ. Sci. Technol.* 26 (5) (1992) 896–901.
- [18] A.A. Keller, M.J. Blunt, P.V. Roberts, Micromodel observation of the role of oil layers in three-phase flow, *Transpl. Porous Media* 26 (1997) 277–297.
- [19] C. Khachikian, T.C. Harmon, Nonaqueous phase liquid dissolution in porous media: current state of knowledge and research needs, *Transpl. Porous Media* 38 (1–2) (2000) 3–28.
- [20] T.-J. Kim, C.V. Chrysikopoulos, Mass transfer correlations for nonaqueous phase liquid pool dissolution in saturated porous media, *Water Resour. Res.* 35 (2) (1999) 449–459.
- [21] K.Y. Lee, C.V. Chrysikopoulos, Numerical modeling of three-dimensional contaminant migration from dissolution of multicomponent NAPL pools in saturated porous media, *Environ. Geol.* 26 (1995) 157–165.
- [22] K.Y. Lee, C.V. Chrysikopoulos, NAPL pool dissolution in stratified and anisotropic porous formations, *J. Environ. Eng. ASCE* 124 (9) (1998) 851–862.
- [23] K.Y. Lee, C.V. Chrysikopoulos, Dissolution of a well-defined trichloroethylene pool in saturated porous media: experimental results and model simulations, *Water Res.* 36 (2002) 3911–3918.
- [24] F.J. Leij, M.T. van Genuchten, Analytical modeling of nonaqueous phase liquid dissolution with Green's functions, *Transpl. Porous Media* 38 (1–2) (2000) 141–166.
- [25] D.M. Mackay, P.V. Roberts, J.A. Cherry, Transport of organic contaminants in groundwater: distribution and fate of chemicals in sand and gravel aquifers, *Environ. Sci. Technol.* 19 (5) (1985) 384–392.

- [26] A.R. Mason, B.H. Kueper, Numerical simulation of surfactant-enhanced solubilization of pooled DNAPL, *Environ. Sci. Technol.* 30 (1996) 3205–3215.
- [27] J.R. Mihelcic, R.G. Luthy, Sorption and microbial degradation of naphthalene in soil water suspensions under denitrification conditions, *Environ. Sci. Technol.* 25 (1991) 169–177.
- [28] S.E. Powers, L.M. Abriola, W.J. Weber Jr., An experimental investigation of nonaqueous phase liquid dissolution in saturated subsurface systems: transient mass transfer rates, *Water Resour. Res.* 30 (2) (1994) 321–332.
- [29] F. Schwillé, *Dense Chlorinated Solvents in Porous and Fractured Media* (J.F. Pankow, Trans.), Lewis Publishers, Chelsea, MI, 1988, 146 pp.
- [30] E.A. Seagren, B.E. Rittman, A.J. Valocchi, An experimental investigation of NAPL-pool dissolution enhancement by flushing, *J. Contam. Hydrol.* 37 (1999) 111–137.
- [31] M.E. Tatalovich, K.Y. Lee, C.V. Chrysikopoulos, Modeling the transport of contaminants originating from the dissolution of DNAPL pools in aquifers in the presence of dissolved humic substances, *Transpl. Porous Media* 38 (1–2) (2000) 93–115.
- [32] E.T. Vogler, C.V. Chrysikopoulos, Dissolution of nonaqueous phase liquid pools in anisotropic aquifers, *Stochastic Environ. Res. Risk Assess.* 15 (2001) 33–46.
- [33] D. Zhou, L.A. Dillard, M.J. Blunt, A physically based model of dissolution of nonaqueous phase liquids in the saturated zone, *Transpl. Porous Media* 39 (2000) 227–255.
- [34] J. Zhu, J.F. Sykes, Stochastic simulations of NAPL mass transport in variably saturated heterogeneous porous media, *Transpl. Porous Media* 39 (2000) 289–314.